USCAP

Check for updates

ARTICLE

M1 macrophage-derived exosomes transfer miR-222 to induce bone marrow mesenchymal stem cell apoptosis

Yanyan Qi[1,2], Tingting Zhu[1], Tingting Zhang[1], Xi Wang[1], Wenbo Li[1], Dongchang Chen[1], Hua Meng[1] and Songtao An[1 ✉]

In the myocardial infarction microenvironment, the effect of macrophages on the function of bone marrow mesenchymal stem cells (BMSCs) is unclear. In this study, we investigated the role of hypoxia/serum deprivation (H/SD)-induced M1-type macrophage-derived exosomes on BMSC viability, migration, and apoptosis. We found that H/SD reduced BMSC viability and migration, increased BMSC apoptosis, and induced macrophage polarization toward the M1 phenotype. BMSCs were cultured by the supernatant of H/SD-induced THP-1 cells (M1-type macrophages) with or without exosome inhibitor treatment. The results show that BMSC apoptosis is increased in the H/SD-induced THP-1 cell supernatant group and is decreased by GM4869 treatment, indicating that M1-type macrophages induce BMSC apoptosis through exosomes. In addition, we confirm that miR-222 plays an important role in promoting BMSC apoptosis by targeting B-cell lymphoma (Bcl)-2. M1-type macrophage-derived exosomes significantly decrease BMSC viability and migration and increase BMSC apoptosis, and these effects are partly abolished by a miR-222 inhibitor. Our findings suggest that under H/SD conditions, exosomes derived from M1-type macrophages can induce BMSC apoptosis by delivering miR-222 to BMSCs.

INTRODUCTION

After acute myocardial infarction (AMI), cardiomyocyte apoptosis and necrosis cannot be effectively ameliorated, resulting in myocardial remodeling and leading to the development of heart failure [1]. To reduce scar tissue formation and stimulate cardiac tissue regeneration, mesenchymal stem cells (MSCs) were used after AMI and showed benefits for cardiac function [2]. Recent data indicated that MSCs are effective in the treatment of AMI by affecting cell differentiation, migration, angiogenesis, and myocardial repair, but the survival and differentiation of stem cells are affected by the local microenvironment, including inflammation, hypoxia, and other factors. Only 1% of bone marrow mesenchymal stem cells (BMSCs) can survive for approximately 4 days after transplantation, and cardiac function can be improved by approximately 3% [3].

The function of MSCs in vivo is closely associated with their surrounding microenvironment. Research shows that myocardial cells [4], cytokines [5], and immune cells (such as Tregs [6] and DCs [7]) in the immune AMI microenvironment can affect the survival and repair functions of MSCs. Macrophages are important immune cells in the AMI microenvironment. Macrophage subpopulations are essential for infarct repair with or without stem cell therapy. Some of the protective effects of MSCs on infarct repair are mediated by macrophages, which are essential for early healing and repair [8]. After AMI, a large number of monocytes gather at the infarcted and surrounding myocardium and then differentiate into macrophages. Macrophages can be divided into the M1 type, which has proinflammatory effects, and the M2 type, which has anti-inflammatory effects. In AMI, macrophages are mainly the M1 type. MSCs can induce macrophages to polarize to the M2 type, thus improving AMI damage [9, 10]. In turn, macrophages also affect MSCs [11, 12]. Do macrophages in the AMI microenvironment also affect the therapeutic effects of MSCs? What is the mechanism that affects MSCs?

Exosomes (Exos) are secreted by eukaryotic cells and are rich in protein, lipids, and RNA. Exos are considered to be important mediators of paracrine signaling [13] through the transfer of miRNAs and other substances to achieve cell communication and regulation [14]. For example, M1-type macrophage-derived exosomes inhibit angiogenesis by transferring miR-155 to endothelial cells and exacerbate cardiac dysfunction in AMI mice [15]. MiR-222 is highly expressed in the exosomes of M1-type THP-1 cells and RAW264.7 cells [16]. The expression of miR-222 is high in myocardial infarction and cardiac decay environments, suggesting that M1 macrophage-derived exosomes may affect the function of MSCs by transferring miR-222.

Target gene prediction analysis shows that miR-222 can inhibit the anti-apoptotic gene Bcl-2 [17]. Therefore, we hypothesized that M1 macrophages secrete exosomes and transfer miR-222 to MSC to inhibit the expression of the antiapoptotic gene Bcl-2, thus promoting MSC apoptosis and inhibiting MSC proliferation and migration.

MATERIALS AND METHODS
Cell culture
The human monocytic leukemia cell line THP-1 was cultured and maintained in complete RPMI-1640 (Gibco) supplemented with 10% FBS

---

[1]Department of Cardiology, Henan Provincial People's Hospital, Zhengzhou University People's Hospital, 7 Weiwu Road, Zhengzhou, China. [2]Department of Anesthesiology, Henan Provincial People's Hospital, Zhengzhou University People's Hospital, 7 Weiwu Road, Zhengzhou, China. ✉email: ansongtao2020@163.com

and 1% penicillin/streptomycin. THP-1 cells were differentiated into macrophages by treatment with 100 nM PMA (Sigma) for 24 h, and then the adherent M0-type macrophages were cultured in H/SD conditions, which polarized these cells toward the M1 phenotype. BMSCs were cultured in complete RPMI-1640 supplemented with 15% FBS (Gibco) in a humidified atmosphere with 5% CO_2 at 37 °C. To evaluate the effect of THP-1 supernatant or THP-1-derived exosomes on BMSC viability, migration, and apoptosis in vitro, a coculture model was established.

Hypoxia/serum deprivation (H/SD)
H/SD injury was induced under hypoxic stress in BMSCs or THP-1 cells. Cells treated with fresh complete medium and maintained under normoxic conditions (95% air−5% CO_2) were considered the control group. Cells treated with fresh complete medium for 24 h and then exposed to hypoxia (approximately 95% N_2 and 5% CO_2) in an anaerobic system (Thermo Forma) at 37 °C for 24 h were considered the H/SD injury group.

Coculture experiment
For the coculture experiment, we seeded BMSCs in Transwell inserts, and once the cultures reached 70–80% confluence, we added THP-1 cell medium (with or without GW4869) or THP-1-derived exosomes and then placed the cultures in H/SD conditions for 24 h. BMSC viability, migration, and apoptosis were evaluated by CCK-8 assay, crystal violet staining, and flow cytometry, respectively.

Oligonucleotide transfection and lentivirus infection
Synthetic miRNA mimics, inhibitors, and negative control oligonucleotides were designed and produced by RiboBio (Guangzhou, China). Lentiviruses (LV-NC and LV-Bcl-2) were purchased from GenePharma (Shanghai, China). BMSCs were transfected with miRNA using transfection reagents according to the manufacturer's protocols. Briefly, transfection or infection was conducted when the cells reached 50–60% confluence. Total RNA and proteins were obtained after 24 and 48 h, respectively.

BMSC viability assays
CCK-8 assays were used to measure BMSC viability. The cells were seeded on 96-well flat-bottom plates at a density of 2000 cells/well, followed by sample treatment. After incubation, 10 μL of CCK-8 solution was added to the medium. The absorbance (OD) value was measured at 450 nm using a microplate reader.

BMSC migration assays
A two-chamber Transwell system with an 8-μm pore size was used in these assays. BMSCs were seeded into the upper chamber of the inserts in a serum-free medium, while medium containing 10% FBS, THP-1 cell supernatant, or THP-1-derived exosomes, was added to the lower chamber. After incubation for 12 h, the inserts were fixed with 100% methanol and subsequently stained with 0.1% crystal violet. The migrated cells on the lower side of the inserts were imaged and counted.

Flow cytometric analysis of apoptosis and macrophage cell proportions
BMSC apoptosis induced by H/SD was assessed using flow cytometry with Annexin-V-FITC/PI dual staining. The green fluorescence of annexin-V and red fluorescence of PI were measured by a flow cytometer. The amounts of early apoptosis, late apoptosis, and necrosis were determined as the percentages of annexin-V+/PI−, annexin-V+/PI+, and annexin-V−/PI+ cells, respectively.

Analysis of CD206+Arg-1+ and iNOS+CD11c+ cell proportions among THP-1 cells was performed. After treatment, THP-1 cells were counted and incubated for 45 min at 4 °C. PE-conjugated CD11c and CD206 antibodies (BD Biosciences) were added and incubated for 45 min, and the cells were washed and further incubated with Alexa Fluor 594-conjugated iNOS and FITC-conjugated Arg-1 (BD Biosciences), respectively, for 45 min at 4 °C. iNOS+CD11c+ macrophages were regarded as M1 macrophages, and CD206+Arg-1+ macrophages were regarded as M2 macrophages.

Enzyme-linked immunosorbent assay (ELISA)
The levels of various cytokines (TNF-α, IL-10, and IL-1β) in THP-1 cell supernatant were measured using commercial ELISA kits (Abcam, Cambridge, UK) according to the manufacturer's protocol.

Real-time PCR analysis
Total RNA was extracted from cells or exosomes using TRIzol reagent (Sangon, Shanghai, China). For miR-222 detection, the isolated RNA was reverse-transcribed using the miRNA qRT-PCR Starter Kit (RiboBio, China), and U6 was used as the internal control. For iNOS, Arg-1, and Bcl-2 mRNA analysis, qRT-PCR was performed with SYBR1 Green PCR Master Mix (Applied Biosystems, USA), and GAPDH was used as the internal control. RT-PCR was performed on a 7500 Fast Real-Time PCR System according to the manufacturer's instructions. The fold change in gene expression was calculated as $2^{-\Delta\Delta CT}$.

Western blot analysis
BMSCs were seeded in plates and incubated until they reached 70–80% confluence at 37 °C in a 5% CO_2 incubator. Stimulation was applied as the indicated time. Then, the cells were washed with PBS and lysed in RIPA lysis buffer containing protease inhibitors. Proteins were extracted, separated by SDS-PAGE, and transferred to PVDF membranes. Before being probed with HRP-conjugated secondary antibodies for 1 h at room temperature, the membranes were blocked with 5% nonfat milk and incubated with the indicated primary antibodies at 4 °C overnight. Primary antibodies against Bcl-2 (ab182858), Bax (ab32503), cleaved Caspase-3 (ab32042), iNOS (ab178945) and Arg-1 (ab133543) were used in this study according to the manufacturer's instructions. Signals were captured using an ECL kit. β-actin was used as the internal control. ImageJ software was used to perform densitometric analysis to quantitate the relative protein expression.

Isolation and characterization of THP-1-Exos
Exosomes were extracted from THP-1 cell supernatant by differential centrifugation. Exosome-free FBS (Gibco) was used to culture THP-1 cells to avoid contamination with FBS-derived exosomes. Briefly, the supernatant was collected and further centrifuged to remove dead cells and cell debris. The resultant exosome pellets were resuspended in PBS and prepared for subsequent analysis. The isolated exosomes were washed once with PBS and resuspended for further characterization.

The morphologic characteristics of THP-1-Exos were observed by transmission electron microscopy (TEM). The size distribution of THP-1-Exos was evaluated by Nanosizertechnology (Malvern Instruments, UK). The protein levels of the exosomal surface markers CD63 and Hsp70 were examined by western blotting.

Exosome labeling and uptake
THP-1 cells were transfected with FAM-miR-222, and exosomes were extracted from THP-1 cells as described previously. The exosomes were then labeled with a Dil fluorescent labeling kit (Sigma-Aldrich) according to the manufacturer's instructions. Briefly, 400 μL of Dil was added to the exosome suspension. After incubation for 5 min, an equal volume of exosome-free bovine serum albumin was added to stop the reaction. Subsequently, the exosomes were washed twice with PBS to remove any unbound dye. BMSCs were incubated with Dil-labeled exosomes for 24 h. Images were captured using a confocal microscope.

Luciferase reporter assays
For the reporter assays, 1×10^4 cells in a 96-well plate were transfected with the miR-222 mimic or NC (RiboBio). The cells were then cotransfected with the wild-type or mutant Bcl-2 or Bcl-2 3′UTR. Forty-eight hours later, luciferase activity was measured by the Dual-Luciferase® Reporter Assay System (Promega, Madison, WI, USA) according to the manufacturer's instructions.

Statistical analysis
Statistical results expressed in the figures are shown as the mean ± standard deviation and were calculated from at least three independent experiments. All statistical analyses were performed by GraphPad Prism. Comparisons between two groups were performed by Student's t-tests. One-way ANOVA with post hoc analysis was used for multiple comparisons between ≥3 groups. P values < 0.05 were considered statistically significant.

RESULTS
Hypoxia/serum deprivation (H/SD) inhibits BMSC viability and migration and induces apoptosis
Human BMSCs were cultured in vitro and randomly divided into a normal control group and an H/SD group. H/SD conditions were
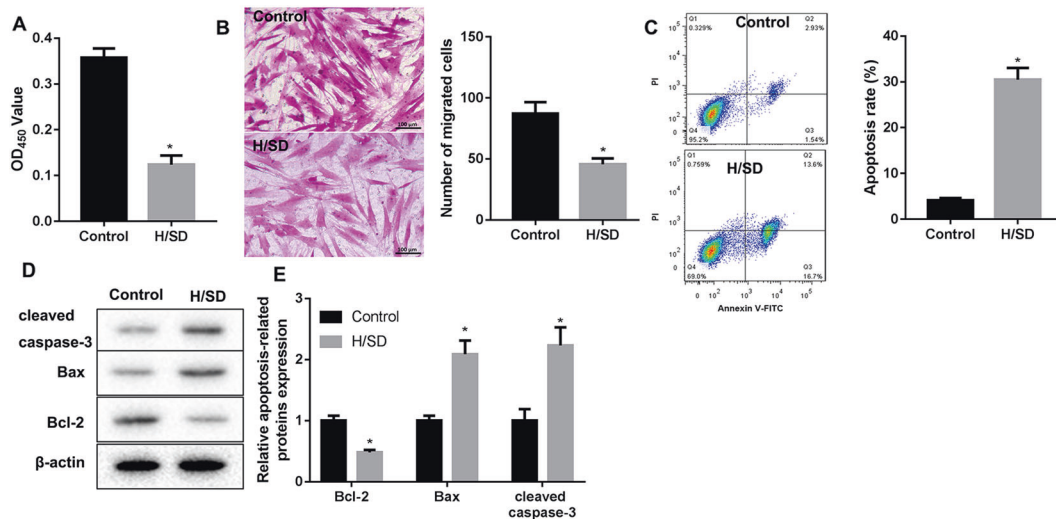
Fig. 1 Hypoxia/serum deprivation (H/SD) induces BMSC apoptosis. Human BMSCs were cultured in vitro and randomly divided into a normal control group (Control) and an H/SD group (H/SD). Hypoxia/serum-deprivation (H/SD) conditions were used to simulate the microenvironment of myocardial infarction. **A** The BMSC viability was measured by CCK-8 assays. **B** The migration of BMSCs was evaluated by Transwell assays. **C** BMSC apoptosis was analyzed by flow cytometry. **D, E**. Apoptotic protein expression was measured by western blotting. *$p < 0.05$ vs the control group.

used to simulate the microenvironment of myocardial infarction. As shown in Fig. 1A, B, the viability and migration of BMSCs in the H/SD group are both significantly lower than those in the control group. The flow cytometry results show that H/SD induces BMSC apoptosis (Fig. 1C). Moreover, the western blot results show an obvious decrease in Bcl-2 and increased Bax and cleaved Caspase-3 expression in the H/SD group (Fig. 1D, E), which further suggests that H/SD induces BMSC apoptosis.

H/SD induces macrophage polarization toward the M1 phenotype

To investigate the effect of H/SD on macrophage polarization, THP-1 cells were cultured in vitro and stimulated with H/SD. A significant increase in the proportion of M1-type macrophages and no significant change in M2-type macrophages indicate that H/SD induces macrophage polarization toward the M1 phenotype (Fig. 2A). Then, the expression of the M1- and M2-type macrophage markers iNOS and Arg-1, respectively, was measured by RT-qPCR and western blotting. As shown in Fig. 2B, E, the mRNA and protein expression of the M1-type macrophage marker iNOS is upregulated in the H/SD group, while there is no significant change in the expression of the M2-type macrophage marker Arg-1. In addition, the M1- or M2-type macrophage cytokines TNF-α, IL-1β, and IL-10 were evaluated by ELISA (Fig. 2F, H). The results show that the secretion of the M1-type macrophage cytokines TNF-α and IL-1β is increased in the H/SD group, while there is no significant change in the secretion of the M2-type macrophage cytokine (IL-10). These data suggest that H/SD induces macrophage polarization toward the M1 phenotype.

M1-type macrophages inhibit BMSC viability and migration and induce BMSC apoptosis

H/SD induced THP-1 cell polarization toward the M1 phenotype. Next, to investigate the effect of M1-type macrophages on viability, migration, and apoptosis, BMSCs were cultured with supernatant collected from THP-1 cells in the control group and H/SD group, followed by H/SD. As shown in Fig. 3A, B, the viability and migration of BMSCs in the supernatant of THP-1 cells from the H/SD group are significantly lower than those in the control group. The flow cytometry results show that the supernatant from

H/SD-induced THP-1 cells induces BMSC apoptosis (Fig. 3C). These data indicate that under H/SD conditions, the supernatant from M1-type macrophages inhibits BMSC viability and migration and induces BMSC apoptosis.

Furthermore, to verify that M1-type macrophage supernatant influences BMSC function through exosomes, exosome inhibitor (GM4869) or DMSO were added to H/SD-induced THP-1 cells. Then, BMSCs were cultured with the supernatant collected from THP-1 cells treated with DMSO or GM4869, followed by H/SD. As shown in Fig. 3D, E, the viability and migration of BMSCs in the supernatant of THP-1 cells treated with GM4869 are significantly lower than those in the DMSO group. The flow cytometry results show that GM4869-treated THP-1 cell supernatant induces BMSC apoptosis (Fig. 3F). These data indicate that under H/SD conditions, M1-type macrophages inhibit BMSC viability and migration and induce BMSC apoptosis through exosomes.

Effects of M1-type macrophage-derived exosomes on the viability, migration, and apoptosis of BMSCs

To investigate the effect of macrophage-derived exosomes on the function of BMSCs, the supernatants of THP-1 cells in the normal control group and H/SD group were collected, and exosomes produced by THP-1 cells were isolated and named M0-Exos and M1-Exos, respectively. We extracted exosomes by ultracentrifugation, and transmission electron microscopy was used to identify the quality of the isolated exosomes (Fig. 4A). Data from Nanosight analysis confirm that the average exosome size is consistent (Fig. 4B). Western blot analysis reveals that the extracted exosomes are positive for two different exosome markers (CD63 and Hsp70) (Fig. 4C), indicating that M0-Exos and M1-Exos have been isolated.

Next, BMSCs were randomly divided into three groups: the PBS incubation group (Control), the M0-Exo incubation group (M0-Exo), and the M1-Exo incubation group (M1-Exo). BMSCs were cultured with Exos, followed by H/SD. As shown in Fig. 4D, E, the viability and migration of BMSCs in the M1-Exo treatment group are significantly lower than those in the M0-Exo group. The flow cytometry results show that M1-Exos induce BMSC apoptosis (Fig. 4F). Therefore, our findings suggest that under H/SD conditions, M1-type macrophages inhibit BMSC viability and migration and induce BMSC apoptosis through exosomes.
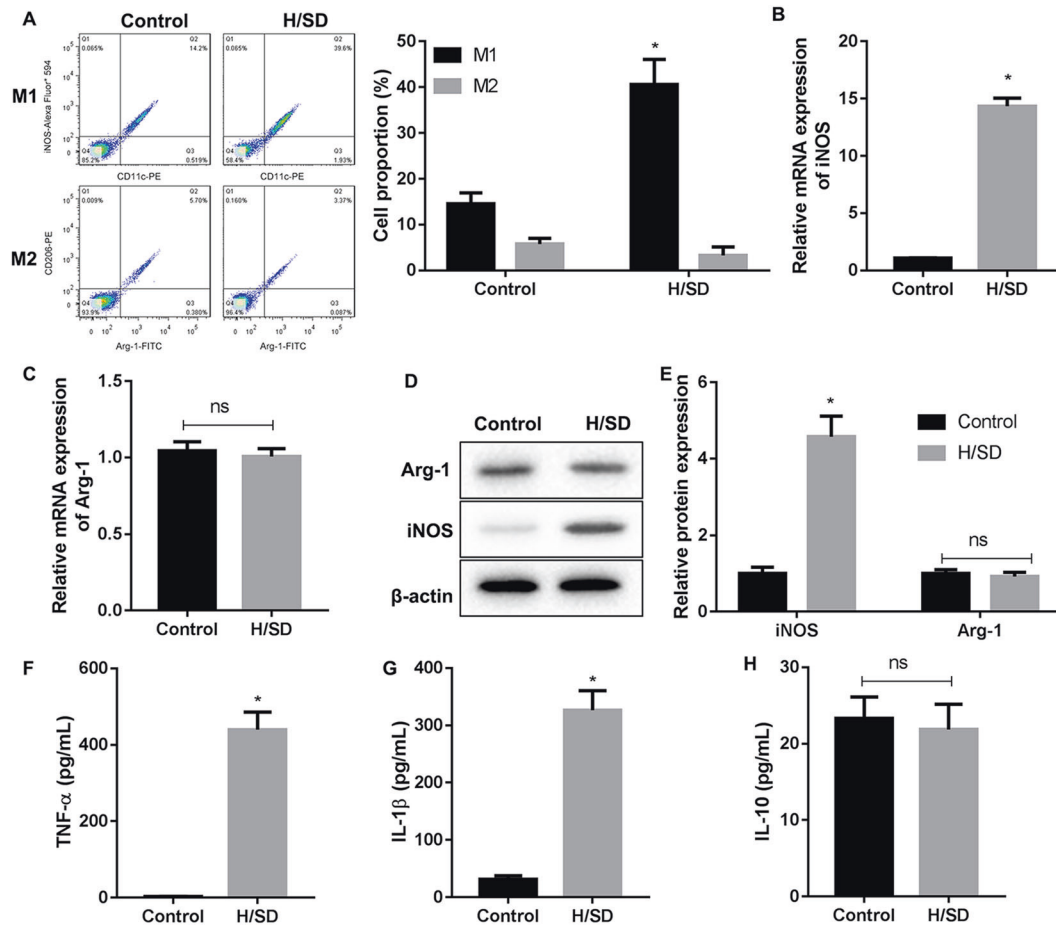
Fig. 2 H/SD induces macrophage polarization toward the M1 phenotype. THP-1 cells were cultured in vitro and randomly divided into a normal control group and an H/SD group. H/SD conditions were used to simulate the microenvironment of myocardial infarction. **A** The proportion of M1- and M2-type macrophages was analyzed by flow cytometry. **B, C** The mRNA expression of iNOS and Arg-1 was measured by RT-qPCR. **D, E** The protein expression of iNOS and Arg-1 was measured by western blotting. **F, H** The TNF-α, IL-1β, and IL-10 levels were evaluated by ELISA. *$p < 0.05$ vs the control group.

M1-type macrophages transport miR-222 via exosomes to affect the viability, migration, and apoptosis of BMSCs

As shown in Fig. 5A, miR-222 is expressed at significantly high levels in M1-Exos. To further explore the effect of M1 macrophages on BMSC viability, migration, and apoptosis through miRNAs in exosomes, the inhibitor NC and miR-222 inhibitor were transfected into THP-1 cells, and exosomes were extracted from the transfected THP-1 cells and named M1-Exos-NC and M1-Exos-miR-222I, respectively. The RT-PCR results show that the expression level of miR-222 in the M1-Exo-miR-222I group is significantly downregulated relative to that in the M1-Exo-NC group (Fig. 5B). Next, BMSCs were randomly divided into 4 groups: the normal control group (Control), the M1-Exo incubation group (M1-Exo), the M1-Exo-NC incubation group (M1-Exo-NC), and the M1-Exo-miR-222I incubation group (M1-Exo-miR-222I). BMSCs were cultured with Exos, followed by H/SD. RT-PCR analysis indicates that miR-222 in BMSCs is strongly upregulated in the M1-Exo group, but is downregulated in the M1-Exo-miR-222I group (Fig. 5C). As shown in Fig. 5D, E, both the viability and migration of BMSCs in the M1-Exo treatment group are significantly reduced, while inhibiting miR-222 attenuates the effect of M1-Exos on viability and migration. The flow cytometry results show that M1-Exos induce BMSC apoptosis, and compared to that of the M1-Exo-NC group, the apoptosis rate is decreased in the M1-Exo-miR-222I group (Fig. 5F). Finally, to assess whether M1-Exos regulated BMSC function in vitro by transferring miR-222, we isolated exosomes from FAM-miR-222-transfected THP-1 cells, labeled the

resultant exosomes with Dil, and then added them to BMSCs. FAM-miR-222 signals were green and Dil was red. Nuclei were stained with Hoechst 33342 (blue) (Fig. 5G). The results indicate that under H/SD conditions, M1-type macrophages inhibit BMSC viability and migration and induce BMSC apoptosis through miR-222 in exosomes.

M1 macrophage-derived exosomes deliver miR-222 to inhibit Bcl-2 protein expression and induce BMSC apoptosis

By binding to sequences in the 3′ UTRs of genes, miRNAs can inhibit target mRNAs by translational suppression and mRNA destabilization. TargetScan was used to predict the potential target of miR-222. We found a highly conserved and specific binding sequence between miR-222 and the Bcl-2 3′UTR (Fig. 6A). Our results show that the miR-222 mimic significantly inhibits luciferase activity when cotransfected with the reporter and the WT-Bcl-2 3′UTR but without the MUT-Bcl-2 3′UTR (Fig. 6B). The mRNA and protein expression of Bcl-2 is also downregulated in BMSCs transfected with the miR-222 mimic, but is upregulated in BMSCs transfected with the miR-222 inhibitor (Fig. 6C, D), which further demonstrated the direct binding of miR-222 to the Bcl-2 3′UTR. Then, BMSCs were cotransfected with the miR-222 mimic and LV-Bcl-2, followed by H/SD stimulation.

Vascular endothelial growth factor (VEGF) and hepatocyte growth factor (HGF) are cardioprotective by increasing the tolerance of cardiomyocytes to ischemia, reducing cardiomyocyte
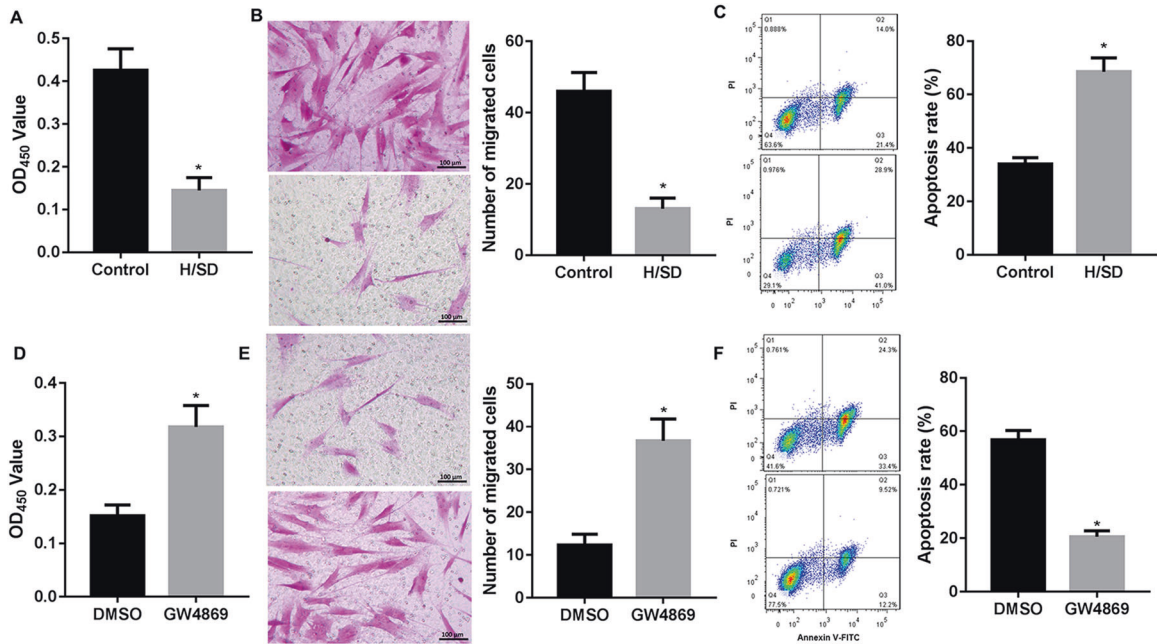
Fig. 3   Effects of M1-type macrophages on the viability, migration, and apoptosis of BMSCs. BMSCs were cultured with the supernatant collected from THP-1 cells in the control group and H/SD group, followed by H/SD. **A** BMSC viability was measured by CCK-8 assays. **B** The migration of BMSCs was evaluated by Transwell assays. **C** BMSC apoptosis was analyzed by flow cytometry. BMSCs were cultured with the supernatant collected from THP-1 cells in the H/SD group and treated with DMSO or the exosome inhibitor GM4869 (10 μm), followed by H/SD. **D** BMSC viability was measured by CCK-8 assays. **E** The migration of BMSCs was evaluated by Transwell assays. **F** BMSC apoptosis was analyzed by flow cytometry. *$p < 0.05$ vs the control or DMSO group.
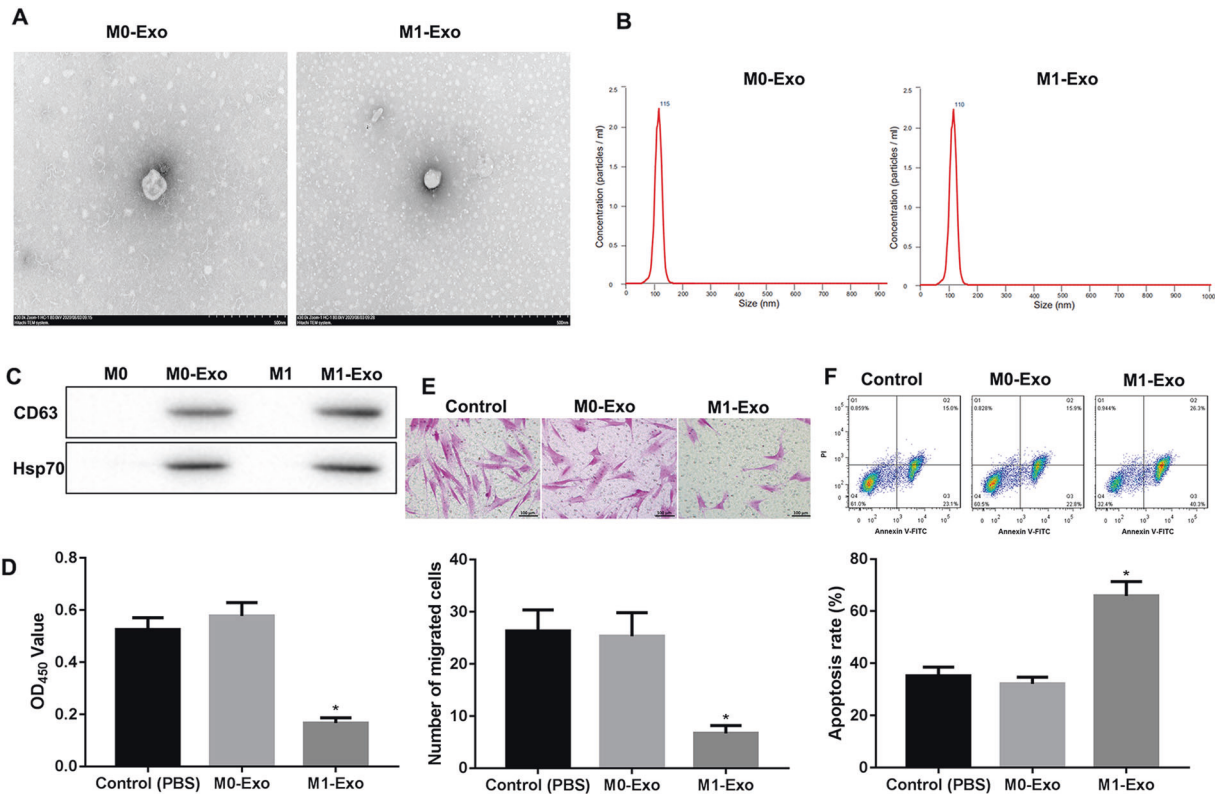
Fig. 4   Effects of M1-type macrophage-derived exosomes on the viability, migration, and apoptosis of BMSCs. The supernatants of THP-1 cells from the normal control group and H/SD group were collected. The exosomes were extracted from THP-1 cells and named M0-Exos and M1-Exos. **A** Electron microscopic images of M0-Exos and M1-Exos. **B** Quantification of M0-Exos and M1-Exos using NTA. **C** Measurement of exosomal markers (Hsp70 and CD63) by western blotting. BMSCs were randomly divided into three groups: PBS incubation group (Control), M0-Exo incubation group (M0-Exo), and M1-Exo incubation group (M1-Exo). BMSCs were cultured with Exos, followed by H/SD. **D** BMSC viability was measured by CCK-8 assays. **E** The migration of BMSCs was evaluated by Transwell assays. **F** BMSC apoptosis was analyzed by flow cytometry. *$p < 0.05$ vs the M0-Exo group.
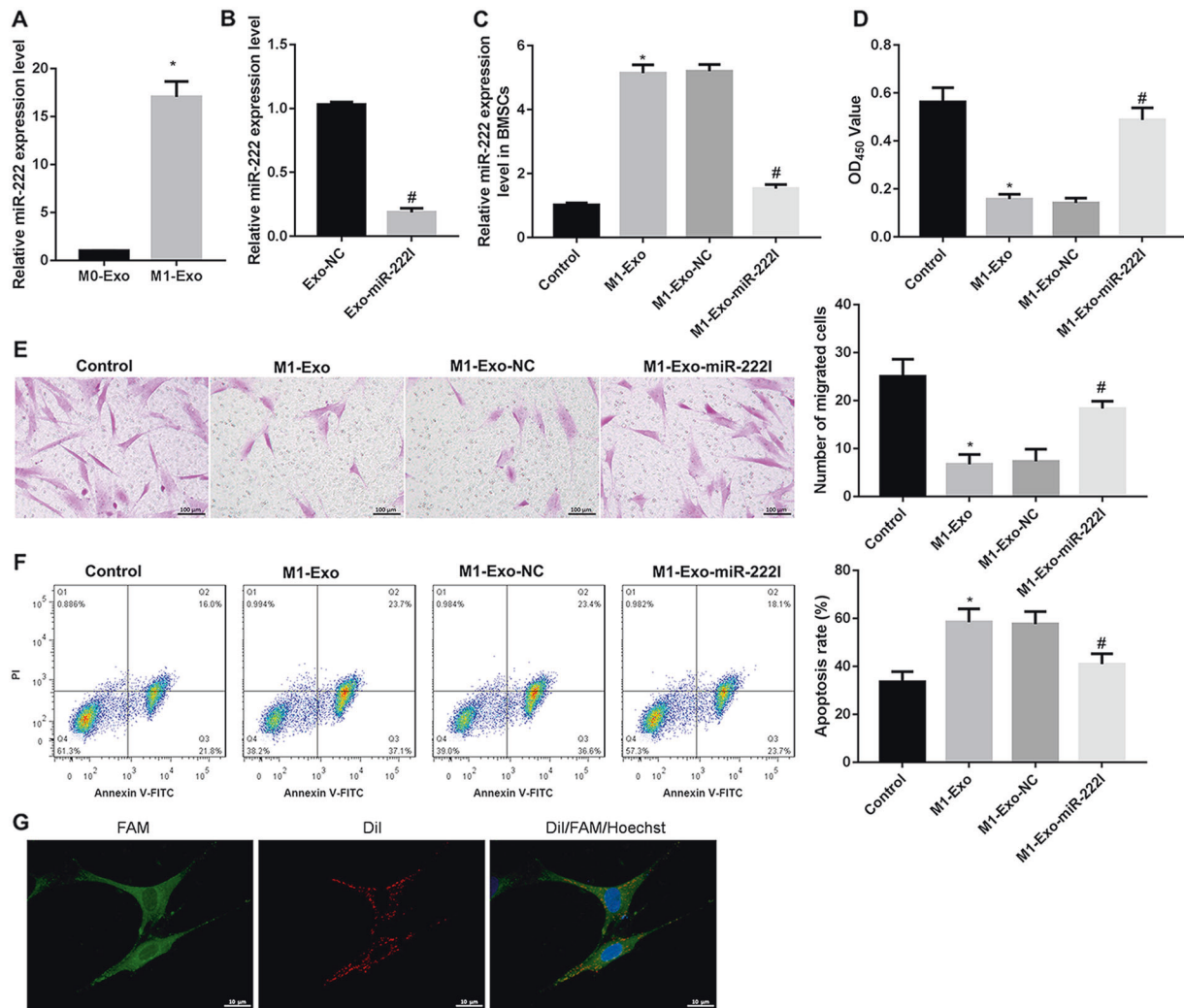
Fig. 5 **M1-type macrophages transport miR-222 through exosomes to affect the viability, migration, and apoptosis of BMSCs. A** The miR-222 expression level in M0-Exos and M1-Exos was measured by RT-qPCR. BMSCs were randomly divided into four groups: normal control group (Control), M1-Exo incubation group (M1-Exo), M1-Exo-NC incubation group (M1-Exo-NC), and M1-Exo-miR-222I incubation group (M1-Exo-miR-222I). BMSCs were cultured with Exos, followed by H/SD. In the M1-Exo-NC group and M1-Exo-miR-222I group, the inhibitor NC and miR-222 inhibitor were transfected into THP-1 cells, and exosomes were extracted from transfected THP-1 cells and named M1-Exos-NC and M1-Exos-miR-222I, respectively. **B** The miR-222 expression level in M1-Exos-NC and M1-Exos-miR-222I was measured by RT-qPCR. **C** The miR-222 expression level in BMSCs was measured by RT-qPCR. **D** BMSC viability was measured by CCK-8 assays. **E** The migration of BMSCs was evaluated by Transwell assays. **F** BMSC apoptosis was analyzed by flow cytometry. **G** FAM-labeled miR-222 (shown in green) and Dil-labeled macrophage-derived exosomes (shown in red). The uptake of miR-222 in macrophage-derived exosomes by BMSCs was observed under a laser-scanning confocal microscope. $*p < 0.05$ vs the M0-Exo or control group; $^{\#}p < 0.05$ vs the inhibitor NC group.

apoptosis, and increasing prosurvival Akt activation. Therefore, we have measured the concentration of VEGF and HGF in each group of cells. The results show that miR-222 mimic significantly reduces the levels of VEGF and HGF in BMSCs, and overexpression of Bcl-2 increases their concentration (Supplementary Fig. 1), suggesting that BMSCs exert beneficial effects against myocardial infarction by secreting VEGF and HGF. The significantly reduced OD value and number of migrated cells indicate the decreased viability and migration induced by the miR-222 mimic, which are increased again, indicating the opposing effect of LV-Bcl-2 on BMSC viability and migration (Fig. 6E, G). In contrast to the effect on viability and migration, the BMSC apoptosis rate is increased in the miR-222 mimic transfection group and decreased in the miR-222 mimic and LV-Bcl-2 cotransfection group (Fig. 6H, I), suggesting the opposite effect of LV-Bcl-2 on BMSC apoptosis.

In addition, BMSCs were transfected with LV-Bcl-2, followed by M1-Exo treatment and H/SD. both the OD value and the number of migrated cells are increased (Fig. 6J, L), and apoptosis is

decreased (Fig. 6E, G) in the LV-Bcl-2 group, but these results are all reversed by M1-Exos, suggesting that M1-Exos reverse the effect of LV-Bcl-2 on BMSC viability, migration, and apoptosis. In summary, these data show that under H/SD conditions, M1 macrophage exosome-mediated transfer of miR-222 induces BMSC apoptosis by targeting Bcl-2.

DISCUSSION
BMSCs have the potential to differentiate into various cell types, and their transplantation is effective for the treatment of AMI-associated diseases [18]. H/SD conditions were used to simulate the microenvironment of myocardial infarction. Consistent with the results reported in other studies [19, 20], H/SD induced BMSC apoptosis and reduced cell viability and migration. Apoptosis, also known as programmed cell death, is triggered via two major signaling pathways, the extrinsic (death receptor-mediated) and intrinsic (mitochondria-dependent) pathways. Caspases, a family
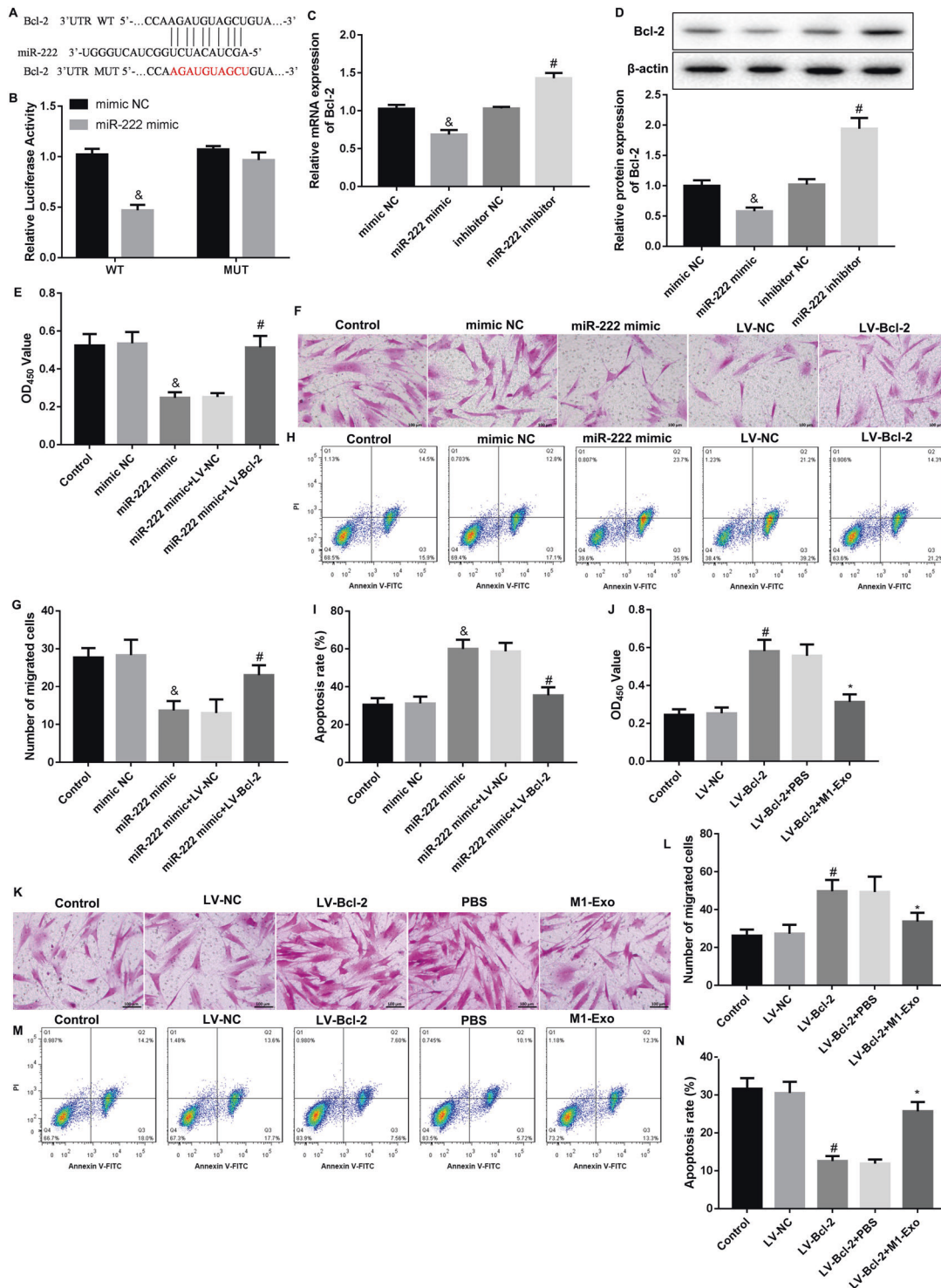
Fig. 6 M1 macrophage-derived exosomes deliver miR-222 to inhibit Bcl-2 protein expression and induce BMSC apoptosis. A Schematic illustration of the miRNA-binding sites of miR-222 in Bcl-2. **B** The direct binding of miR-222 to Bcl-2 was analyzed by dual-luciferase reporter assays. **C, D**. BMSCs were transfected with the miR-222 mimic/inhibitor and their control sequences. The mRNA and protein expression of Bcl-2 was measured by qRT-PCR and western blotting, respectively. BMSCs were cotransfected with the miR-222 mimic and LV-Bcl-2, followed by H/SD. **E** BMSC viability was measured by CCK-8 assays. **F, G**. The migration of BMSCs was evaluated by Transwell assays. **H, I** BMSC apoptosis was analyzed by flow cytometry. BMSCs were transfected with LV-Bcl-2, followed by M1-Exo treatment and H/SD. **J** BMSC viability was measured by CCK-8 assays. **K, L** The migration of BMSCs was evaluated by Transwell assays. **M, N**. BMSC apoptosis was analyzed by flow cytometry. $\&p < 0.05$ vs the mimic NC group; $\#p < 0.05$ vs the inhibitor NC or LV-NC group.

of intracellular cysteine endopeptidases, are responsible for cellular apoptosis via the extrinsic pathway. In our study, we found that H/SD upregulated the expression of cleaved caspase-3, which consequently increased BMSC apoptosis.

Myocardial infarction can trigger a strong inflammatory response, which is characterized by the infiltration of inflammatory cells into the damaged heart. Many kinds of inflammatory cells can not only repair injury but also exacerbate ischemic injury. Among them, macrophages are numerous and valuable immune cells that play important roles in myocardial infarction. In this study, H/SD conditions were used to simulate the microenvironment of myocardial infarction. We observe a significantly increased proportion of M1-type macrophages, upregulated expression of iNOS, and enhanced TNF-α and IL-1β levels in THP-1 cells under H/SD conditions, but there is no significant change in the proportion of M2-type macrophages, Arg-1 expression, or IL-10 level, which indicates that H/SD induce macrophage polarization toward the M1 phenotype. In cerebral infarction, M1 macrophages peak at 3 d after myocardial infarction and are decreased until 14 d after myocardial infarction, whereas M2 macrophages peak at 7 d after myocardial infarction and are decreased at 14 d after myocardial infarction, indicating that M1 macrophages play a dominant role in the early stage of myocardial ischemia injury, while M2 subtype macrophages account for the majority of cells in the repair process [21]. A recent report shows that M1 macrophages were activated in ischemia −reperfusion injury that was characterized by tissue hypoxia and a limited blood supply [22]. Here, our study demonstrates that H/SD could induce macrophage polarization towards the M1 phenotype, which is consistent with previous reports showing that H/SD increased CD80$^+$ cell counts in primary murine macrophages [23].

A new study suggests that the responses of macrophage (macrophage polarization and the microvesicle secretion by macrophages) modulated environments and weakened the osteogenic ability of BMSCs [24]. Our study shows that H/SD-induced macrophages (M1-type macrophages) could significantly inhibit BMSC viability and migration and increase BMSC apoptosis. An exosome inhibitor (GM4869) was used to evaluate the effect of blocking exosomes on the functions of BMSCs, and the results reveal that H/SD-induced macrophages (M1-type macrophages) inhibit BMSC viability and migration and induce BMSC apoptosis through exosomes. Consistent with the literature [24], our results indicate that the macrophage-mediated microenvironment has adverse effects on the function of BMSCs in the context of H/SD, which may be associated with the inflammatory response and weakening the homing ability of BMSCs.

Exosomes can mediate intercellular communication and regulation by transferring miRNAs [14]. MiR-222 expression in H/SD-induced macrophages (M1-type macrophages) is markedly higher than that in M0 macrophages, which is consistent with the research report by Wang et al [16]. Then, we prove the targeted relationship between miR-222 and Bcl-2 by luciferase reporter assays, which is consistent with the reported literature [17]. After transfecting the inhibitor NC and miR-222 inhibitor into THP-1 cells, we collected THP-1 cell-derived exosomes, BMSC was cultured with these exosomes. The results show that exosomes derived from H/SD-induced macrophages (M1-type macrophages) affect the function of BMSCs by transferring miR-222 to recipient cells. Finally, through a series of rescue experiments, we further prove that under H/SD conditions, M1-type macrophage-derived exosomes deliver miR-222 to inhibit Bcl-2 protein expression and induce BMSC apoptosis.

Myocardial cell death is one of the characteristics of myocardial infarction. Both mitochondrial apoptotic pathway and inflammatory response can lead to cardiomyocyte death, and anti-apoptotic and antioxidant are proved to reduce the damage of cardiomyocytes [25]. The above experimental results show that M1-type macrophage-derived exosomes deliver miR-222 to inhibit Bcl-2 protein expression and induce BMSC apoptosis. Exosomes transport miRNAs from donor cells to neighboring and distantly related recipient cells. In view of this result, we speculate that M1 macrophage-derived exosome transfer of miR-222 may target cardiomyocytes and induce apoptosis by inhibiting Bcl-2 protein.

In conclusion, our study demonstrates that under H/SD conditions, M1 macrophage-derived exosomes transfer miR-222 to induce BMSC apoptosis. This study provides, at least in part, a molecular basis for further studies on the effect of macrophages on BMSCs to treat AMI in a myocardial infarction microenvironment. Collectively, our results suggest that in the myocardial infarction microenvironment, macrophage delivery of miR-222 via exosomes has adverse effects on the function of BMSCs, which will affect the efficacy of BMSCs in the treatment of AMI.

DATA AVAILABILITY
The datasets generated and/or analyzed during the current study are not publicly available but are available from the corresponding author on reasonable request.

REFERENCES
1. Goedemans L, Bax J, Delgado V. COPD and acute myocardial infarction. Eur Respir Rev. 2020;29:190139.
2. Miao C, Lei M, Hu W, Han S, Wang Q. A brief review: the therapeutic potential of bone marrow mesenchymal stem cells in myocardial infarction. Stem Cell Res Ther. 2017;8:242.
3. Khodayari S, Khodayari H, Amiri A, Eslami M, Farhud D, Hescheler J, et al. Inflammatory microenvironment of acute myocardial infarction prevents regeneration of heart with stem cells therapy. Cell Physiol Biochem. 2019;53:887–909.
4. Hu M, Guo G, Huang Q, Cheng C, Xu R, Li A, et al. The harsh microenvironment in infarcted heart accelerates transplanted bone marrow mesenchymal stem cells injury: the role of injured cardiomyocytes-derived exosomes. Cell Death Dis. 2018;9:357.
5. Chen Y, Zuo J, Chen W, Yang Z, Zhang Y, Hua F, et al. The enhanced effect and underlying mechanisms of mesenchymal stem cells with IL-33 overexpression on myocardial infarction. Stem Cell Res Ther. 2019;10:295.
6. Zhou Y, Singh A, Hoyt R, Wang S, Yu Z, Hunt T, et al. Regulatory T cells enhance mesenchymal stem cell survival and proliferation following autologous cotransplantation in ischemic myocardium. J Thorac Cardiovasc Surg. 2014;148:1131–7.
7. Silva AM, Almeida MI, Teixeira JH, Maia AF, Calin GA, Barbosa MA, et al. Dendritic cell-derived extracellular vesicles mediate mesenchymal stem/stromal cell recruitment. Sci Rep. 2017;7:1667.
8. Ben-Mordechai T, Holbova R, Landa-Rouben N, Harel-Adar T, Feinberg M, Abd Elrahman I, et al. Macrophage subpopulations are essential for infarct repair with and without stem cell therapy. J Am Coll Cardiol. 2013;62:1890–901.
9. Cho DI, Kim MR, Jeong HY, Jeong HC, Jeong MH, Yoon SH, et al. Mesenchymal stem cells reciprocally regulate the M1/M2 balance in mouse bone marrow-derived macrophages. Exp Mol Med. 2014;46:e70.
10. Zhao J, Li X, Hu J, Chen F, Qiao S, Sun X, et al. Mesenchymal stromal cell-derived exosomes attenuate myocardial ischaemia-reperfusion injury through miR-182-regulated macrophage polarization. Cardiovasc Res. 2019;115:1205–16.
11. Hotchkiss KM, Clark NM, Olivares-Navarrete R. Macrophage response to hydrophilic biomaterials regulates MSC recruitment and T-helper cell populations. Biomaterials. 2018;182:202–15.
12. Mahon OR, Browe DC, Gonzalez-Fernandez T, Pitacco P, Whelan IT, Von Euw S, et al. Nano-particle mediated M2 macrophage polarization enhances bone formation and MSC osteogenesis in an IL-10 dependent manner. Biomaterials. 2020;239:119833.
13. Hessvik NP, Llorente A. Current knowledge on exosome biogenesis and release. Cell Mol Life Sci. 2018;75:193–208.
14. Yu X, Odenthal M, Fries JW. Exosomes as miRNA carriers: formation-function-future. Int J Mol Sci. 2016;17:2028.
15. Liu S, Chen J, Shi J, Zhou W, Wang L, Fang W, et al. M1-like macrophage-derived exosomes suppress angiogenesis and exacerbate cardiac dysfunction in a myocardial infarction microenvironment. Basic Res Cardiol. 2020;115:22.
16. Wang Z, Zhu H, Shi H, Zhao H, Gao R, Weng X, et al. Exosomes derived from M1 macrophages aggravate neointimal hyperplasia following carotid artery injuries in mice through miR-222/CDKN1B/CDKN1C pathway. Cell Death Dis. 2019;10:422.
17. Wang W, Wang J, Zhang J, Taq W, Zhang Z. miR-222 induces apoptosis in human intervertebral disc nucleus pulposus cells by targeting Bcl-2. Mol Med Rep. 2019;20:4875–82.
18. Haddad K, Potter B, Matteau A, Reeves F, Leclerc G, Rivard A, et al. Analysis of the COMPARE-AMI trial: first report of long-term safety of CD133+ cells. Int J Cardiol. 2020;319:32–35.

1326

19. Gong X, Fan G, Wang W, Wang G. Trimetazidine protects umbilical cord mesenchymal stem cells against hypoxia and serum deprivation induced apoptosis by activation of Akt. Cell Physiol Biochem. 2014;34:2245–55.
20. Wang F, Zhou H, Du Z, Chen X, Zhu F, Wang Z, et al. Cytoprotective effect of melatonin against hypoxia/serum deprivation-induced cell death of bone marrow mesenchymal stem cells in vitro. Eur J Pharmacol. 2015;748:157–65.
21. Liu W, Zhang X, Zhao M, Zhang X, Chi J, Liu Y, et al. Activation in M1 but not M2 macrophages contributes to cardiac remodeling after myocardial infarction in rats: a critical role of the calcium sensing receptor/NRLP3 inflammasome. Cell Physiol Biochem. 2015;35:2483–2500.
22. Ye L, He S, Mao X, Zhang Y, Cai Y, Li S. Effect of hepatic macrophage polarization and apoptosis on liver ischemia and reperfusion injury during liver transplantation. Front Immunol. 2020;11:1193.
23. Zhang F, Xuan Y, Cui J, Liu X, Shao Z, Yu B. Nicorandil modulated macrophages activation and polarization via NF-κb signaling pathway. Mol Immunol. 2017;88:69–78.
24. Chen L, Qiao P, Liu H, Shao L. Amorphous calcium phosphate NPs mediate the macrophage response and modulate BMSC osteogenesis. Inflammation. 2021;44:278–96.
25. Zhang J, Liu D, Zhang M, Zhang Y. Programmed necrosis in cardiomyocytes: mitochondria, death receptors and beyond. Br J Pharmacol.2019;176:4319–39.

AUTHOR CONTRIBUTIONS
Y. Q. performed study concept and design; Y. Q., T. Z., T. Z., X. W., W. L., and D. C. performed development of methodology and writing, review, and revision of the paper; H. M. and S. A. provided acquisition, analysis and interpretation of data, and statistical analysis; H. M. provided technical and material support. All authors read and approved the final paper.

CONFLICT OF INTEREST
The authors declare no competing interests.

ADDITIONAL INFORMATION
Supplementary information The online version contains supplementary material available at https://doi.org/10.1038/s41374-021-00622-5.

Correspondence and requests for materials should be addressed to S.A.

Reprints and permission information is available at http://www.nature.com/reprints

Publisher's note Springer Nature remains neutral with regard to jurisdictional claims in published maps and institutional affiliations.